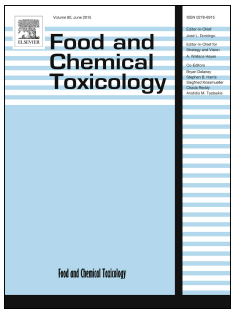

Facile synthesis of Cu NPs@Fe_3O_4-lignosulfonate: Study of catalytic and antibacterial/antioxidant activities

Zahra Nezafat, Mohammad Mahdi Karimkhani, Mahmoud Nasrollahzadeh, Shahrzad Javanshir, Abdollah Jamshidi, Yasin Orooji, Ho Won Jang, Mohammadreza Shokouhimehr

PII: S0278-6915(22)00508-7

DOI: https://doi.org/10.1016/j.fct.2022.113310

Reference: FCT 113310

To appear in: *Food and Chemical Toxicology*

Received Date: 18 April 2022

Revised Date: 7 July 2022

Accepted Date: 14 July 2022

Please cite this article as: Nezafat, Z., Karimkhani, M.M., Nasrollahzadeh, M., Javanshir, S., Jamshidi, A., Orooji, Y., Jang, H.W., Shokouhimehr, M., Facile synthesis of Cu NPs@Fe_3O_4-lignosulfonate: Study of catalytic and antibacterial/antioxidant activities, *Food and Chemical Toxicology* (2022), doi: https://doi.org/10.1016/j.fct.2022.113310.

Author Contributions: Zahra Nezafat: Visualization, Validation, Writing - original draft, Formal Analysis, Investigation, Mohammad Mahdi Karimkhani: Visualization, Validation, Writing - original draft, Formal Analysis, Investigation, Mahmoud Nasrollahzadeh: Supervision, Visualization, Validation, Writing - review and editing, Resources, Formal Analysis, Shahrzad Javanshir: Supervision, Resources, Conceptualization, Investigation, Abdollah Jamshidi: Supervision, Conceptualization, Investigation, Yasin Orooji: Conceptualization, Methodology, Writing: Original Draft, Project administration, Ho Won Jang: Conceptualization, Investigation, Formal Analysis, Mohammadreza Shokouhimehr: Project administration, Fund Acquisition, Analysis.

Facile synthesis of Cu NPs@Fe_3O_4-lignosulfonate: Study of catalytic and antibacterial/antioxidant activities

Zahra Nezafat, Mohammad Mahdi Karimkhani, Mahmoud Nasrollahzadeh,* Shahrzad Javanshir, Abdollah Jamshidi, Yasin Orooji,* Ho Won Jang and Mohammadreza Shokouhimehr

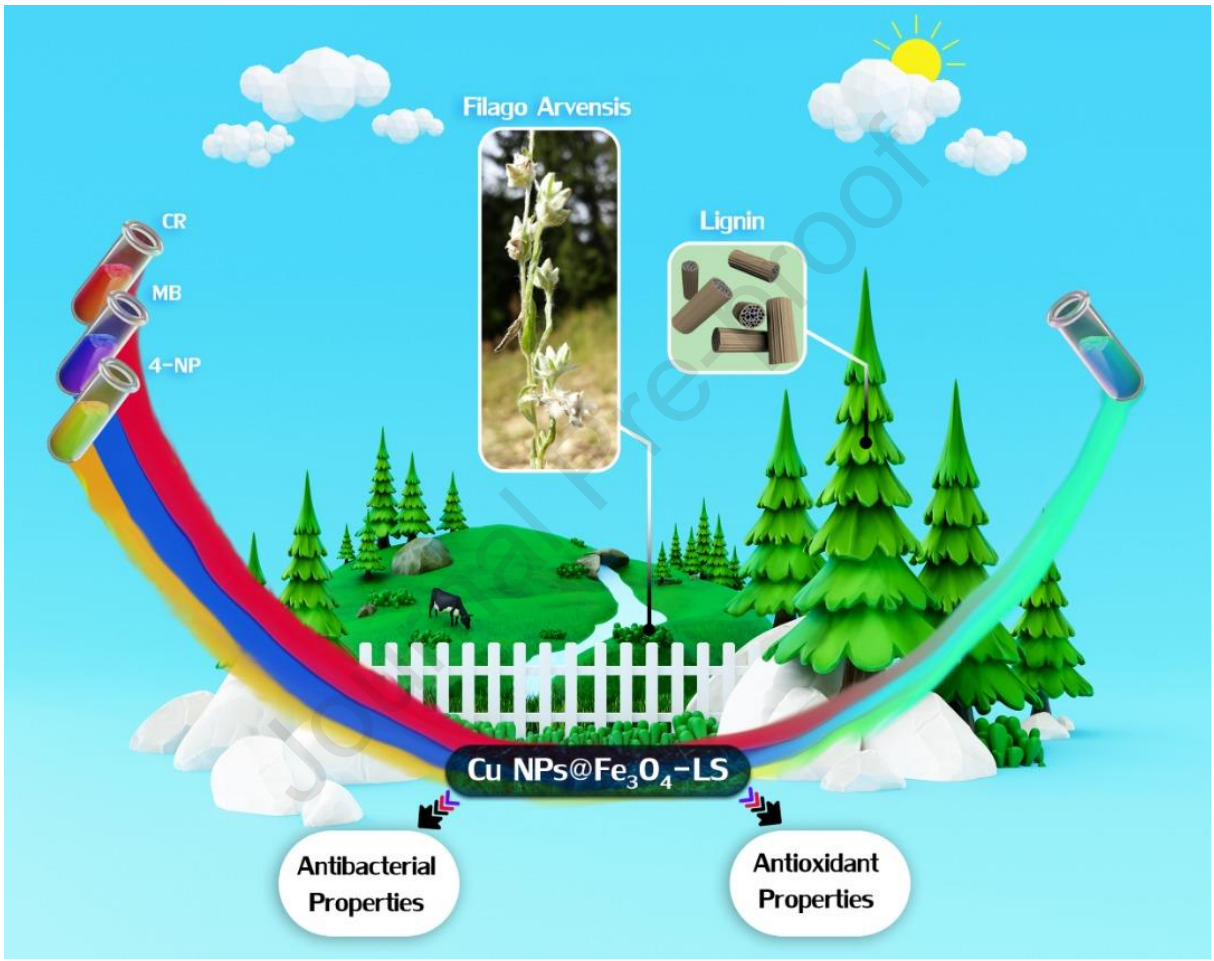

*E-mail: mahmoudnasr81@gmail.com (M. Nasrollahzadeh).

*E-mail: Yasin Orooji (orooji@zjnu.edu.cn).

Facile synthesis of Cu NPs@Fe_3O_4-lignosulfonate: Study of catalytic and antibacterial/antioxidant activities

Zahra Nezafat,[a] Mohammad Mahdi Karimkhani,[b] Mahmoud Nasrollahzadeh,[c,*] Shahrzad Javanshir,[a] Abdollah Jamshidi,[b] Yasin Orooji,[d,*] Ho Won Jang[e] and Mohammadreza Shokouhimehr[e]

[a]*Pharmaceutical and Heterocyclic Chemistry Research Laboratory, Department of Chemistry, Iran University of Science and Technology, Tehran 16846-13114, Iran*

[b]*Department of Food Hygiene and Aquaculture, Faculty of Veterinary Medicine, Ferdowsi University of Mashhad, Mashhad, Iran*

[c]*Department of Chemistry, Faculty of Science, University of Qom, Qom 37185-359, Iran*

[d]*College of Geography and Environmental Sciences, Zhejiang Normal University, Jinhua 321004, China*

[e]*Department of Materials Science and Engineering, Research Institute of Advanced Materials, Seoul National University, Seoul 08826, Republic of Korea*

Abstract

Environmental pollution is one of the important concerns for human health. There are different types of pollutants and techniques to eliminate them from the environment. We hereby report an efficient method for the remediation of environmental contaminants through the catalytic reduction of the selected pollutants. A green method has been developed for the immobilization of copper nanoparticles on magnetic lignosulfonate (Cu NPs@Fe_3O_4-LS) using the aqueous extract of *Filago*

[*]*E-mail*: mahmoudnasr81@gmail.com (M. Nasrollahzadeh).

[*]*E-mail*: Yasin Orooji (orooji@zjnu.edu.cn).

arvensis L. as a non-toxic reducing and stabilizing agent. The characterization of the prepared Cu NPs@Fe_3O_4-LS was achieved by vibrating sample magnetometer (VSM), Fourier-transform infrared spectroscopy (FT-IR), transmission electron microscopy (TEM), high resolution TEM (HRTEM), X-ray diffraction (XRD), scanning TEM (STEM), thermogravimetry-differential thermal analysis (TG/DTA), fast Fourier transform (FFT), energy-dispersive X-ray spectroscopy (EDS), and X-ray photoelectron (XPS) analyses. The synthesized Cu NPs@Fe_3O_4-LS was applied as a magnetic and green catalyst in the reduction of Congo Red (CR), 4-nitrophenol (4-NP), and methylene blue (MB). The progress of the reduction reactions was monitored by UV-Vis spectroscopy. Finally, the biological properties of the Cu NPs@Fe_3O_4-LS were investigated. The prepared catalyst demonstrated excellent catalytic efficiency in the reduction of CR, 4-NP, and MB in the presence of sodium borohydride ($NaBH_4$) as the reducing agent. The appropriate magnetism of Cu NPs@Fe_3O_4-LS made its recovery very simple. The advantages of this process include a simple reaction set-up, high and catalytic antibacterial/antioxidant activities, short reaction time, environmentally friendliness, high stability, and easy separation of the catalyst. In addition, the prepared Cu NPs@Fe_3O_4-LS could be reused for four cycles with no significant decline in performance.

Keywords: Lignosulfonate; Green method; Environmental pollutants; Reduction; Antibacterial; Antioxidant; Catalysis

1. Introduction

Growing human population and intense industrial activities have caused huge pollution in the environment. Environmental pollutants are spread all over the earth including mountains, seas, oceans, *etc*. [1-9]. Organic dyes are broadly applied in different chemical industries such as papers, textiles, paints and plastics. Chemical processes produce large amounts of dyes, which leads to the formation of dye-laden, directly entering the environment [5,8-11]. In addition, nitro compounds have different applications as intermediates in various industries, e.g., pesticides, explosives, pigments, pharmaceuticals, *etc*. [7]. Although organic dyes and nitro compounds have many applications, they are highly toxic and carcinogenic, and many enter the ecosystem and environment [7-9]. In recent years, various methods such as biological, physical and chemical methods have been used to remove these contaminants. One of the most promising approaches for the elimination of various pollutants from the environment is catalytic reduction and degradation [7-12].

In general, the chemical reduction is performed using a reducing agent [13-15]. The compounds are almost such that they can only be reduced by reducing agents, which is thermodynamically possible but not kinetically [13-15]. Generally, the presence of an effective catalyst makes the reactions kinetically feasible [15]. Nanomaterials or nanoparticles are one of the most promising compounds, which can be applied in various fields [13-49]. One of the major problems in the application of nanoparticles as catalysts is the problem of agglomeration and accumulation of nanoparticles, which leads to a decline in their catalytic performance. One of the effective methods to solve this problem is to use solid supports to stabilize nanoparticles [50,51]. For this aim, there are different supports such as zeolite, iron oxide, graphene oxide, carbon-based materials, MOF materials, synthetic and polymeric compounds, *etc*. [5,7-10,52-59].

Lignin, the second most abundant source of biomass, after cellulose, is made from plants and mainly located in the middle lamella of the cell wall, lignin acts as a matrix intimately bound to the polysaccharides in order to ensure the cohesion of the structure [60]. Lignin is the pulp industry by-product. Commonly, there are 4 major kinds of lignin including soda, Kraft, organosolv and lignosulfonate, which can be directly obtained from grasses or woods in pulp manufacturing [61]. Additionally, lignin is the most abundant aromatic biopolymer on earth composed of randomly branched methoxylated phenylpropane units; viz. sinapyl (S), *p*-coumaryl alcohols (H) and coniferyl alcohol (G) and primary monolignols (Figure 1 (a)) [62,63,64]. Due to various functional groups such as COOH, OH and C=O on the surface of lignin, it is considered as a suitable choice for catalytic support, which can support the distribution and deposition of metal nanoparticles (MNPs) [65].

For the synthesis of nanoparticles (NPs), there exist different methods, the most important of which are co-precipitation, hydrothermal synthesis, sol-gel, laser ablation and green methods. Some of these methods have disadvantages, which may lead to the formation of many pollutants in the environment. For example, they use chemical reducing agents to reduce nanoparticles [66]. One of the most promising methods for the fabrication of MNPs or metal oxide NPs is the application of green methods, which use different compounds such as bacteria, fungi, yeasts, natural polymers, plant extracts, *etc*. [67-77]. Recently, the use of plant extracts for the fabrication of MNPs has been highly regarded by researchers. In other words, the stabilization and reduction of metal ions using biomolecules such as polysaccharides, proteins, terpenes, amino acids, saponins, vitamins, alkaloids, and phenolics, which are now known to be present in plant extracts, offers the simplest and most inexpensive approach to the synthesis of MNPs [78,79].

Filago arvensis L. from the family of *Asteraceae* is native to Europe, Asia, and North Africa regions. The main morphological feature, which describes the type of the plants, is its receptacular paleae subtend, which is located downwards and more or less surrounds the female florets. The plant is enriched by many valuable phytochemicals such as saponines, flavonoids, glycosides, alkaloids and tannins. Therefore, in this study the areal parts of *Filago arvensis* L. were applied as the reducing media for the green fabrication of MNPs [80,81].

Here Cu NPs were synthesized using *Filago arvensis* L. aqueous extract and immobilized on the magnetic lignosulfonate for the fabrication of Cu NPs@Fe_3O_4-LS. The prepared Cu NPs@Fe_3O_4-LS were applied in the reduction of pollutants using $NaBH_4$ at ambient temperature. The particle size of Fe_3O_4 on the support was nanoscale and the supported catalyst had magnetic properties, which could be used to separate the suspended catalyst particles from the reaction mixture by a magnet. In addition, the biological and antioxidant activities of Cu NPs@Fe_3O_4-LS were examined. The proposed synthetic system shows remarkable performance in terms of eco-friendliness, simplicity and enhancement of the reaction rate. This study could technically promote the synthesis of lignin-based catalysts, and the potential application of immobilized MNPs in catalysis and wastewater remediation.

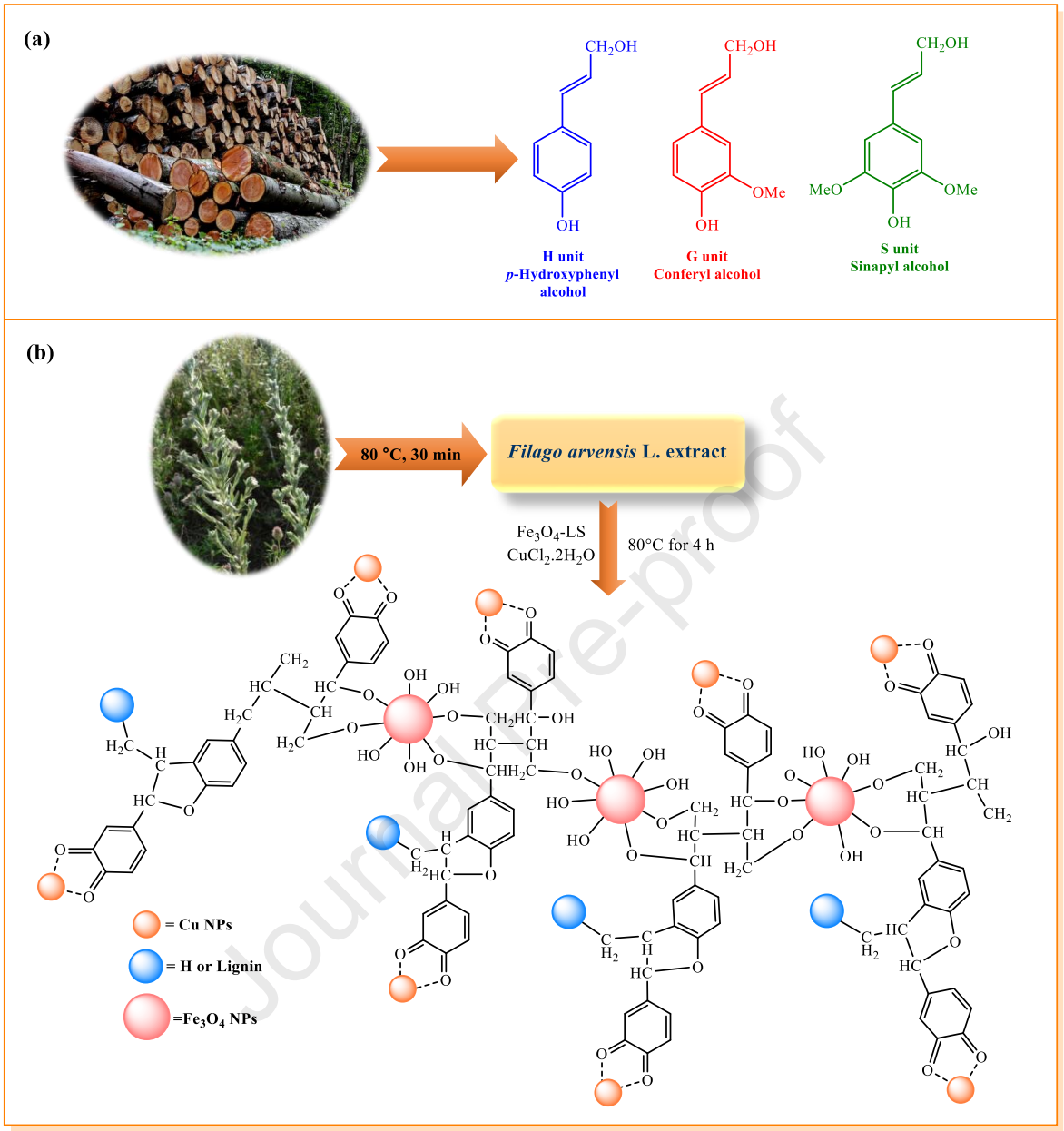

Figure 1. Schematic representation of (a) monomeric units of lignin and (b) pathway for the synthesis of Cu NPs@Fe_3O_4-LS.

2. Experimental

2.1. Apparatuses and chemicals

All chemical compounds were obtained from Sigma-Aldrich Chemical Co. and used without any further purification. Fe_3O_4 NPs were purchased from the Iranian Nanomaterials Pioneer Company

(Mashhad, Iran). FT-IR spectra were recorded using KBr pellets on a Varian model 640 spectrophotometer (Agilent Technologies, Santa Clara, CA, USA). The progress of the reduction of CR, MB and 4-NP was monitored by UV-Vis spectroscopy (UV-Vis, JASCO V-630, Japan). The TEM and XRD analyses were carried out using JEM-2100 (JEOL Ltd., Japan) and Philips powder diffractometer, type PW 1373 goniometer (Philips, Amsterdam, The Netherlands), respectively. In addition, the VSM, TG/DTA and XPS analyses were performed using Lake shore VSM-7410 magnetometer at 298 K (USA), STA 1500 Rheometric-Scientific Company (STA 1500+ Model, England) and PHI 5000 VersaProbe system (ULVAC-PHI, Japan), respectively.

2.2. Preparation of *Filago arvensis* L. aqueous extract

100 g of dried and crushed leaves of the *Filago arvensis* L. and 500 mL of distilled water were mixed at 80 °C for 0.5 h. The obtained aqueous extract was separated, cooled and kept for the fabrication of Cu NPs.

2.3. Biosynthesis of Cu NPs

In a 250 mL flask, 50 mL of the *Filago arvensis* L. extract were added to an aqueous solution of $CuCl_2.2H_2O$ (50 mL, 0.005 M) and the mixture obtained was magnetically stirred at 80 ºC. Cu NPs were formed when the color of the mixture changed to black. Reduction of Cu^{2+} to Cu^0 was finished in 5 min (as checked by UV-Vis spectroscopy). Finally, the synthesized Cu NPs were centrifuged.

2.4. Synthesis of Fe_3O_4-LS

Fe_3O_4-LS was prepared according to a literature method [82]. For this aim, sodium lignosulfonate was first dissolved in dioxane: water (9:1, v/v). A solution of potassium periodate was then added using a peristaltic pump in the dark. Next, Fe_3O_4 NPs were added to the pre-activated sodium lignosulfonate solution over a period of 120 min. The pH and mass ratios were 6.4 and 5:1

respectively. Finally, sodium lignosulfonate was bonded to Fe_3O_4 NPs and the Fe_3O_4-LS was filtered by an external magnet and dried at 110 °C.

2.5. Biosynthesis of Cu NPs@Fe_3O_4-LS

Cu NPs@Fe_3O_4-LS catalyst was synthesized by the addition of Fe_3O_4-LS (1 g) and $CuCl_2.2H_2O$ (0.5 g) in 100 mL of *Filago arvensis* L. aqueous extract and stirring at 80°C for 4 h. Finally, Cu NPs@Fe_3O_4-LS were separated using an external magnet, washed with water and dried (Figure 1 (b)).

2.6 Reduction of MB using Cu NPs@Fe_3O_4-LS

In a beaker, Cu NPs@Fe_3O_4-LS (3.0 mg) was added to MB aqueous solution (25 mL, 3.1×10^{-5} M) and the mixture obtained was then stirred at ambient temperature. 25 mL of 5.3×10^{-3} M $NaBH_4$ solution were then added to the reaction mixture and the reduction progress was followed *via* UV-Vis analysis. At the end, the blue solution became colorless.

2.7 Reduction of CR using Cu NPs@Fe_3O_4-LS

The prowess of Cu NPs@Fe_3O_4-LS in CR reduction at ambient temperature was also examined. In a beaker, an aqueous solution of CR (25 mL, 1.44×10^{-5} M) and 5.0 mg of Cu NPs@Fe_3O_4-LS catalyst was mixed. 25 mL of a newly prepared solution of $NaBH_4$ (5.3×10^{-3} M) was then added to the reaction mixture. The progress of the reduction was followed by UV-Vis analysis. When the reduction was completed, the orange color of the solution changed to colorless.

2.8 Reduction of 4-NP using Cu NPs@Fe_3O_4-LS

For this aim, in a beaker, 25 mL of 4-NP (2.5×10^{-3} M) and 7.0 mg of Cu NPs@Fe_3O_4-LS catalyst was stirred at ambient temperature. 25 mL of freshly prepared solution of $NaBH_4$ (0.25 M) was

then added to the above mixture. At the end, the yellow color of the reaction media changed to colorless.

2.9 Biological studies

The antibacterial activity of Cu NPs@Fe_3O_4-LS was studied using two bacteria viz. *Escherichia coli* (ATCC25922) and *Staphylococcus aureus* (ATCC25923). The antibacterial activity of Cu NPs@Fe_3O_4-LS was studied using the agar disc diffusion technique. A sterile nutrient agar (25 mL) was decanted into a Petri dish and incubated it at 37 °C for 1 day. 100 µL of a suspension comprising of bacteria (1.5×10^8 CFU/mL) extents was placed homogeneously on the agar media surface. A piece of sterile disc was then dipped in Cu NPs@Fe_3O_4-LS suspension (300 µg/mL) and cautiously placed on the agar plate with the smallest distance of 2 cm from each other. The inoculated Petri dishes were incubated for 1 day at 37 °C. The diameter of each zone of inhibition was applied to measure the antibacterial action.

Minimal Inhibitory Concentration (MIC) of Cu NPs@Fe_3O_4-LS was defined by means of the broth dilution technique in a 96-well plate. 100 µL of the Mueller-Hinton Broth culture medium were decanted in each well. 100 µL of different concentrations of Cu NPs@Fe_3O_4-LS were then added into the wells. Finally, 100 µL of a suspension comprising of 5×10^8 CFU/mL of bacteria were distributed in the wells and incubated at 37 °C for 1 day. Gentamicin was a positive control in this experiment. MIC is the lowest concentration required to inhibit bacterial growth. The minimum bactericidal concentration (MBC) indicates the lowest concentration, which kills microorganisms [83].

2.9.1 DPPH free radical scavenging assay

DPPH radical scavenging prowess was calculated according to the results of Karimkhani's research group [84] with minor modifications. About 1 mL of Cu NPs@Fe_3O_4-LS was added to 3 mL of

MeOH and 1 mL of methanolic solution of DPPH radicals (0.012 g/100 mL). The resulting mixture was then stirred and incubated for 2 h at ambient temperature. Finally, the absorbance was recorded at 517 nm *vs*. a blank. The scavenging ability was quantified as follows:

$$\text{Scavenging activity (\%)} = \frac{[(\text{A517nm of control} - \text{A517nm of sample}]}{\text{A517nm of control}} \times 100 \qquad \text{Eq. 1}$$

2.9.2 Reducing power assay

For this purpose, diverse concentrations of Cu NPs@Fe_3O_4-LS in 1.0 mL of deionized water were mixed with phosphate buffer (2.5 mL, 0.2 M, pH = 6.6) and potassium ferricyanide (2.5 mL, 10 g/L). The resulting mixture was then incubated for 30 min at 50 °C. Afterward, a solution of trichloroacetic acid (approximately 2.5 mL, 100 g/L) was added and then the mixture was centrifuged. The supernatant separated by centifugation in the previous step was then mixed with $FeCl_3$ (0.5 mL, 1 g/L) and deionized water (2.5 mL). Finally, the absorbance was recorded at 700 nm. The standard compounds included BHA and BHT. The experiments were carried out in triplicate.

3. Results and discussion

3.1 Characterization of Cu NPs@Fe_3O_4-LS

Cu NPs@Fe_3O_4-LS catalyst was synthesized by an efficient, green and eco-friendly technique using *Filago arvensis* L. aqueous extract as a green reductant. The Cu NPs@Fe_3O_4-LS was characterized by various analyses.

Figure 2 (a) shows the UV-Vis spectra of *Filago arvensis* L. aqueous extract and green synthesized Cu NPs. According to Figure 2(a), the peaks at 358 and 235 nm are due to the presence of cinnamoyl and benzoyl systems in the plant, respectively, which are connected to the transition localized within the ring of these fractions [85]. In other words, these absorption peaks are

associated with the $\pi \rightarrow \pi^*$ transitions and indicate the presence of phenolic fractions, which act as antioxidants for the biosynthesis of NPs, as reported in the literature. When Cu NPs are synthesized, the color of the solution changes to black owing to the excitation of the surface plasmon resonance effect (Scheme S1). The Cu NPs have an absorption peak at 565 nm, which indicates that the green Cu NPs prepared are fairly stable with no clear changes in the position, shape and symmetry of the absorption peak. According to UV-Vis analysis, the formation of Cu NPs through reduction of Cu^{2+} is complete in 5 min and the product is quite stable for 17 days.

To confirm the biosynthesis of Cu NPs and adsorption of phytochemicals on their surface, FT-IR analysis was applied. FT-IR spectroscopy was also used to verify the presence of phenolic compounds and the effects of these biomolecules on the reduction of Cu^{2+} particles to form Cu NPs@Fe_3O_4-LS. In the FT-IR spectrum of Cu NPs (Figure 2(b)), the peaks at 1000-1300, 1491, 1698, and 3510 cm^{-1} are related to C-O, C=C, C=O and OH functional groups, respectively, which confirms the appearance of the flavonoid. Therefore, FT-IR analysis indicates the green fabrication of Cu NPs duo to adsorption of phytochemicals on the Cu nanosurface. In other words, the FT-IR spectrum shows the significant role of the flavonoid (polyphenolic) group in bioactive molecules, which reduce Cu^{2+} metal ions and form Flavonoid@Cu NRs. In the FT-IR of spectrum Cu NPs@Fe_3O_4-LS (Figure 2(c)), the peaks at 3000-3600, 1385, and 1626 cm^{-1} are associated with OH, C=C, and C=O stretching modes, respectively. Surprisingly, the other band at 575 cm^{-1} is attributed to the typical extending vibrations of Fe-O bond. Additionally, the peaks at 1017 and 1070 cm^{-1} are related to the symmetric and asymmetric SO_2 vibrations in lignosulfonate, respectively.

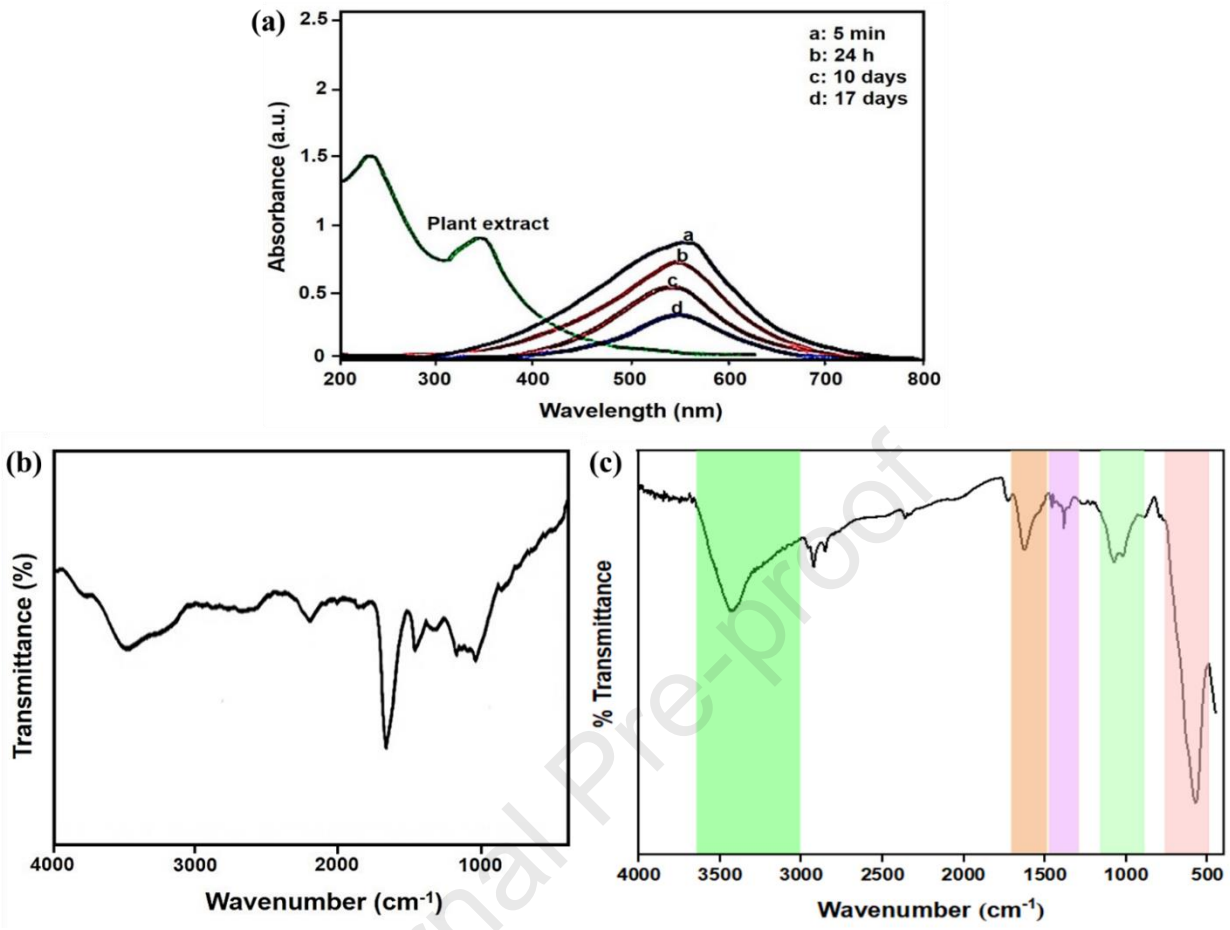

Figure 2. (a) UV-Vis spectra of *Filago arvensis* L. aqueous extract and biosynthesized Cu NPs, FT-IR spectra of (b) Cu NPs and (c) Cu NPs@Fe_3O_4-LS.

Figure 3 (a) shows the XRD pattern of Cu NPs@Fe_3O_4-LS. According to Figure 3 (a), the peaks at 2θ = 30.3°, 35.9°, 43.4°, 54.0°, 57.3°, and 63.2° correspond to the (220), (311), (400), (422), (511), and (440) planes of the cubic Fe_3O_4 (JCPDS 19-0629), respectively [86]. In addition, the XRD pattern displays the structure of the sodium lignosulfonate in noncrystalline phases [87]. The XRD pattern of sodium lignosulfonate shows four major peaks at 23.1°, 25.9°, 27.2°, and 31.5° [87]. Based on the XRD pattern, there are no exact peaks for Cu NPs, indicating the homogeneous dispersion of Cu NPs on Fe_3O_4-LS surface.

The magnetic catalyst can be separated using an external magnet and then reused in the next run [88,89]. The magnetic property of Cu NPs@Fe_3O_4-LS was investigated using VSM analysis (Figure 3 (b)). VSM analysis shows the magnetic property of Cu NPs@Fe_3O_4-LS, enabling them to be simply removed from the reaction media and reused several times.

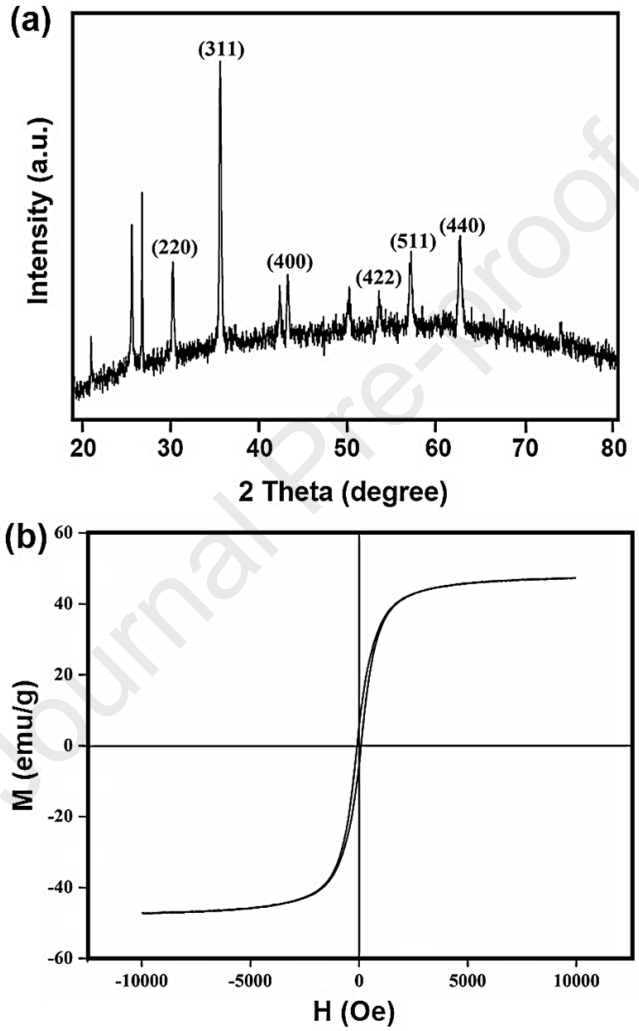

Figure 3. (a) XRD pattern and (b) VSM analysis of Cu NPs@Fe_3O_4-LS.

The size distribution and morphology of Cu NPs@Fe_3O_4-LS have been investigated using TEM analysis. Figure 4 (a-d) represent the TEM images of Cu NPs@Fe_3O_4-LS catalyst. The black particles with larger particle size are due to Fe_3O_4-LS. Additionally, the small spherical dark dots

represent Cu NPs, and it can be observed that they are homogenously dispersed on the support. The average particle size of Cu NPs@Fe_3O_4-LS is 26 nm with spherical morphology.

The HRTEM and fast Fourier transform (FFT) images of Cu NPs@Fe_3O_4-LS shown in Figures 4 (e-g) confirm the highly crystalline structure of Fe_3O_4 and Cu NPs. Furthermore, the STEM image of Cu NPs@Fe_3O_4-LS indicates a homogeneous nanostructured catalyst (Figure 4 (h)).

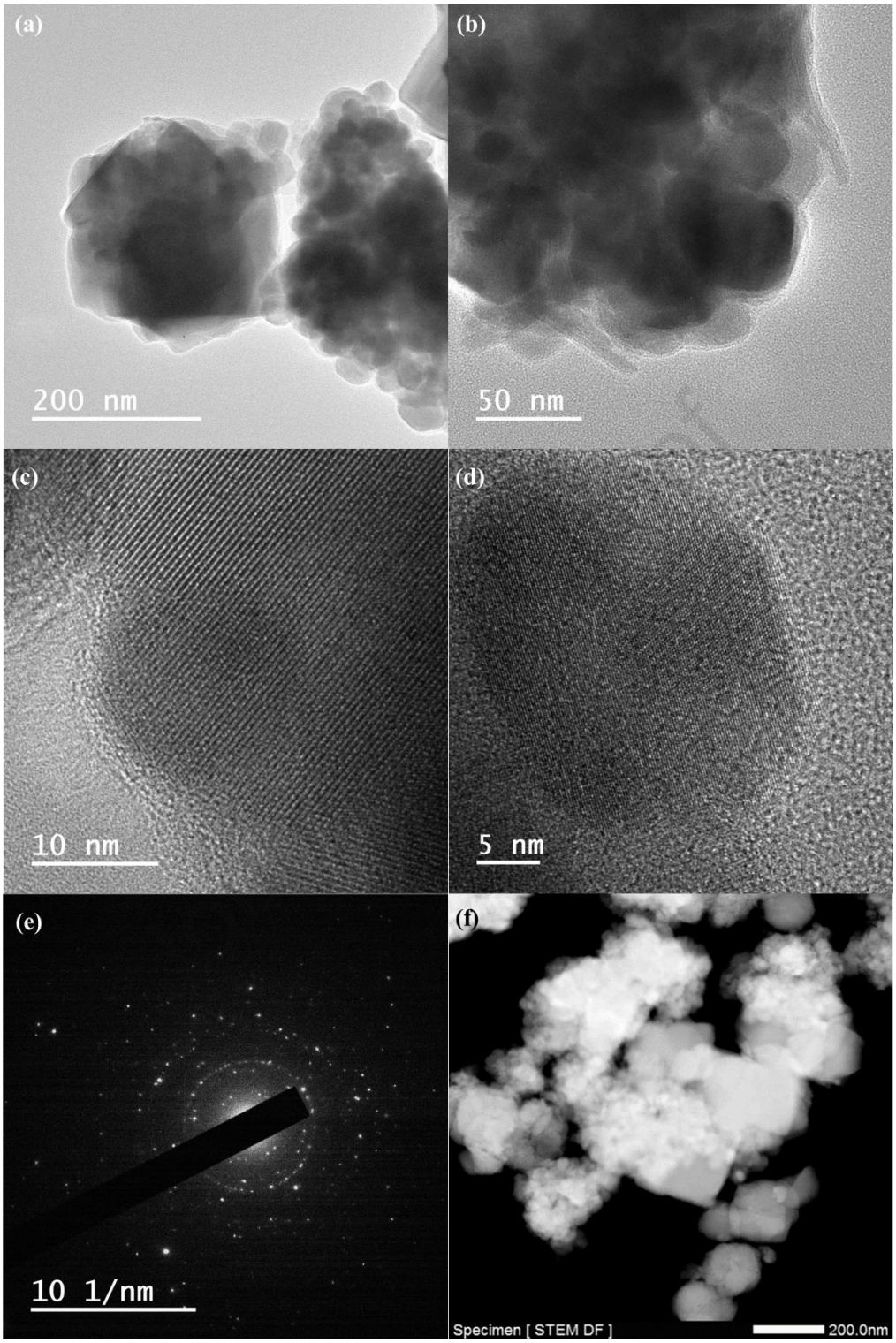

Figure 4. (a, b) TEM, (c, d) HRTEM, (e) FFT, and (f) STEM images of Cu NPs@Fe_3O_4-LS.

The XPS analysis of Cu NPs@Fe_3O_4-LS is displayed in Figure S1. According to Figure S1 (a), the peaks at 711, 283, 531, and 932.7 eV confirm the presence of Fe, C, O, and Cu respectively. Moreover, the peaks at 952.7 and 932.7 eV are due to Cu NPs (Figure S1 (b)) [90].

The thermal stability of Cu NPs@Fe_3O_4-LS was studied in the range of 25-700 °C using TG/DTA analysis (Figure S2). In the initial stage, the loss of weight in the range of 30-100 °C is due to the loss of adsorbed water. In the next stage; that is, 380-550 °C range, mass reduction is expected to occur due to the elimination of organic compound chelated with biosynthesized NPs owing to the increased temperature. At temperatures higher than 550 °C, the loss of weight is related to the decomposition of the catalyst.

Figure S2 shows the EDS and elemental mapping of Cu NPs@Fe_3O_4-LS. Figure S2 confirms the presence of C, Fe, S, Cu, and O in the structure of Cu NPs@Fe_3O_4-LS. Furthermore, elemental mapping indicates that Cu NPs are uniformly dispersed on the catalyst surface. It should be noted that nickel grids have been used for TEM analysis instead of conventional copper grids to clearly confirm the presence of copper in the prepared catalyst. Therefore, the presence of nickel in the EDS spectrum is due to the nickel TEM grid.

3.2 Cu NPs@Fe_3O_4-LS catalyzed MB reduction

Due to the toxic and non-biodegradable nature of dyes [91-98] and to evaluate the catalytic effect of Cu NPs@Fe_3O_4-LS, this catalyst was used in the reduction of MB in the presence of $NaBH_4$ (Scheme 1 (a)). In the absence of Cu NPs@Fe_3O_4-LS, the reduction reaction does not occur (Table 1, entry 1). The effect of the loading Cu NPs@Fe_3O_4-LS heterogeneous catalyst on the reduction of MB dye is shown in Table 1. The reduction of MB was studied in the presence of 1.0 and 3.0 mg of Cu NPs@Fe_3O_4-LS catalyst (Table 1). The results reveal that catalytic activity increases

upon increasing the weight of Cu NPs@Fe_3O_4-LS catalyst from 1.0 to 3.0 mg. According to Figure 5 (a), MB shows an absorption peak at λ_{max}=663 nm. Nonetheless, upon the addition of Cu NPs@Fe_3O_4-LS to the reaction mixture, the reduction of MB occurs and the color of the solution disappears. The change of color was observed using UV-Vis spectroscopy at designated times. When the amount of catalyst is increased from 1.0 to 3.0 mg, the reduction of MB takes place immediately (Table 1, entry 3).

Table 1. MB reduction using different amounts of Cu NPs@Fe_3O_4-LS.

Entry	Cu NPs@Fe_3O_4-LS (mg)	$NaBH_4$ (M)	Time
1	0.0	5.3×10^{-3}	110 min[a]
2	1.0	5.3×10^{-3}	32 s
3	3.0	5.3×10^{-3}	Immediately

[a] No reaction.

3.3 Cu NPs@Fe_3O_4-LS catalyzed reduction of CR

The catalytic prowess of Cu NPs@Fe_3O_4-LS in the reduction of CR aqueous solution was studied (Scheme 1 (b)). In the absence of Cu NPs@Fe_3O_4-LS, the reduction of CR does not occur (Table 2, entry 1). In the presence of the Cu NPs@Fe_3O_4-LS catalyst and $NaBH_4$, the absorption intensity at λ_{max}=493 nm declines with reaction time (Figure 5 (b)), and the solution color disappears, indicating CR reduction. To determine the appropriate amount of Cu NPs@Fe_3O_4-LS catalyst, the reduction of CR was carried out using diverse amounts of Cu NPs@Fe_3O_4-LS catalyst (Table 2).

Table 2. CR reduction using different amounts of Cu NPs@Fe_3O_4-LS.

Entry	Cu NPs@Fe_3O_4-LS (mg)	$NaBH_4$ (M)	Time
1	-	5.3×10^{-3}	100 min[a]
2	3.0	5.3×10^{-3}	60 s
3	5.0	5.3×10^{-3}	40 s

[a] No reaction.

3.4 Cu NPs@Fe_3O_4-LS catalyzed reduction of 4-NP

Furthermore, the catalytic prowess of Cu NPs@Fe_3O_4-LS in 4-NP reduction to 4-aminophenol (4-AP) in the presence of $NaBH_4$ has been investigated (Scheme 1 (c)). According to Figure 5 (c), the absorption band of 4-NP is observed at λ_{max}=317 nm and the solution is yellow in color. However, after the $NaBH_4$ addition, the absorption peak increases from 317 to 400 nm due to 4-nitrophenolate ion (4-NPT) formation in alkaline environment and the color of the solution changes from pale to bright yellow. In the absence of a catalyst, this peak remains constant for a long time without change in intensity. This confirms that $NaBH_4$ alone has no effect on the reduction. Upon the addition of Cu NPs@Fe_3O_4-LS, the intense peak at 400 nm is reduced and the dark yellow color disappears after 180 s. Furthermore, the new at 300 nm confirms the formation of 4-AP. The effect of various amounts of $NaBH_4$ and Cu NPs@Fe_3O_4-LS have been studied (Table 3). In the absence of Cu NPs@Fe_3O_4-LS and $NaBH_4$, the reduction reaction does not occur (Table 3, entry 1). However, in the presence of Cu NPs@Fe_3O_4-LS, a reduction of 100% is achieved. The presence of Cu NPs on the surface of Fe_3O_4-LS, which increases the formation of active hydrogen species on the surface of nanocomposites, could explain the increased reduction efficiency. The variation of the amount of Cu NPs@Fe_3O_4-LS and $NaBH_4$ was studied and it was found that the best results are obtained when 7.0 mg of Cu NPs@Fe_3O_4-LS and 100 equivalents of $NaBH_4$ are used (Table 3, entry 3). In addition, longer reaction times are required using 75 equivalents solution of $NaBH_4$ (Table 3, entries 4 and 5).

311 **Table 3.** 4-NP reduction using Cu NPs@Fe_3O_4-LS and $NaBH_4$.

Entry	Cu NPs@Fe_3O_4-LS (mg)	$NaBH_4$ (equivalents)	Time
1	-	-	160 min[a]
2	5.0	100	5 min
3	7.0	100	3 min
4	5.0	75	10 min
5	7.0	75	8 min

312 [a] No reaction.

313

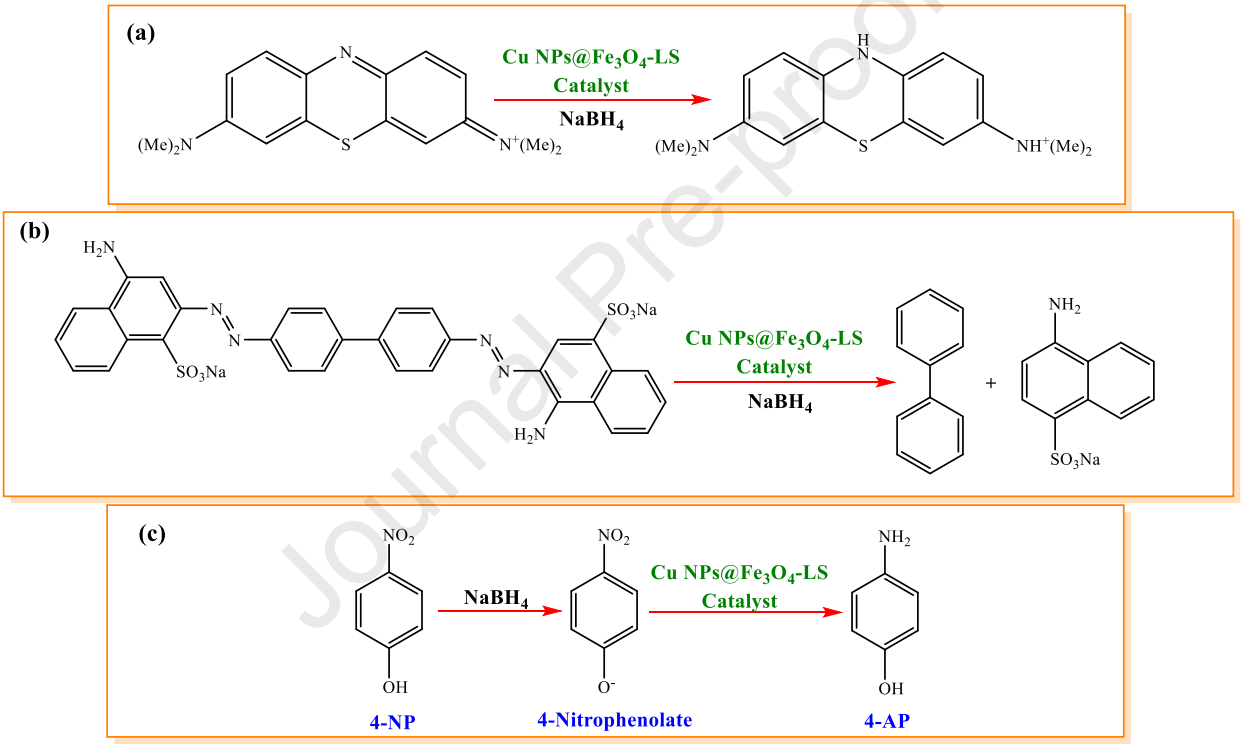

314

315 **Scheme 1.** Reduction of (a) MB, (b) CR and (c) 4-NP using Cu NPs@Fe_3O_4-LS catalyst and

316 $NaBH_4$.

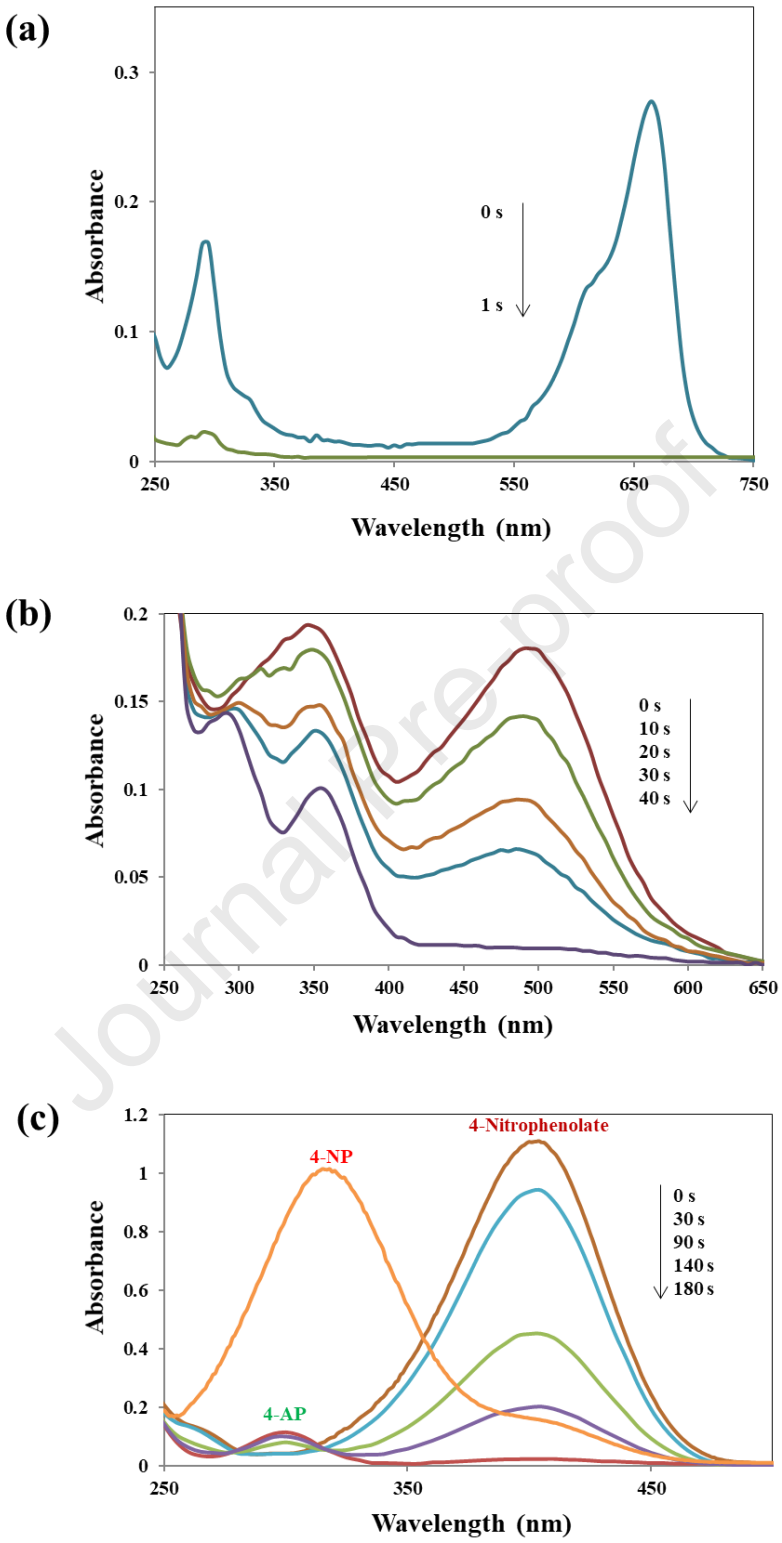

Figure 5. UV-Vis spectra of the reduction of (a) MB, (b) CR and (c) 4-NP.

The proposed mechanism for the reduction of 4-NP shown in Scheme 2 involves the electron transfer (ET) reaction of $NaBH_4$, as a hydrogen donor. The surface of Cu NPs@Fe_3O_4-LS in the presence of borohydride can act as electron donors in catalytic reduction reactions. Fast ET can increase local electron concentration and facilitate ET from BH_4^- (donor) to 4-NP (acceptor) through the nanocomposite, resulting in improved reduction activity. As displayed in Scheme 2, during the reaction, BH_4^- ions and 4-NP are adsorbed on Cu NPs@Fe_3O_4-LS surface *via* electrostatic attraction. As a result, the nitro group of 4-NP is converted into the corresponding amino group through the formation of 4-nitrophenolate intermediate. In addition, Cu NPs immobilized on the Fe_3O_4-LS support plays a noteworthy role in the effectiveness of reduction of 4-NP by $NaBH_4$ *via* electron transfer between BH_4^- donor and nitro group, which acts as an acceptor. In fact, BH_4^- ions react with the composite surface and transfer surface-hydrogen species (which are involved in 4-NP reduction) onto the composite surface. Finally, 4-AP product was separated from Cu NPs@Fe_3O_4-LS surface to free up active sites to continue the process and the catalytic sequence.

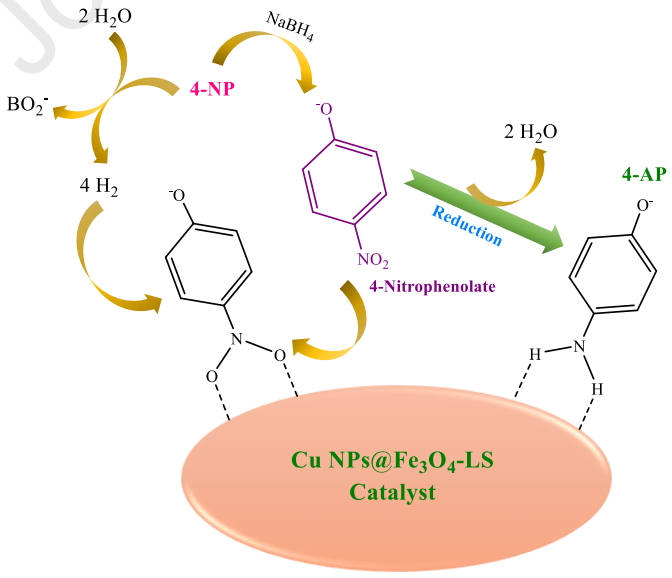

Scheme 2. Proposed mechanism for the reduction of 4-NP.

Due to the fact that the reduction time of MB and CR is very short, it is not possible to calculate the rate constant for these two reduction reactions. However, the rate constant for the reduction of 4-NP has been calculated. Owing to the presence of large excess of $NaBH_4$ compared to 4-NP, the rate of reduction is independent of the concentration of $NaBH_4$ so that the reduction of 4-NP in the presence of Cu NPs@Fe_3O_4-LS can be treated as a pseudo-first-order reaction. The catalytic reduction rate (k) can be determined by plotting. $-\ln(C_t/C_0)$ *vs* the reaction time, t (Figure 6).

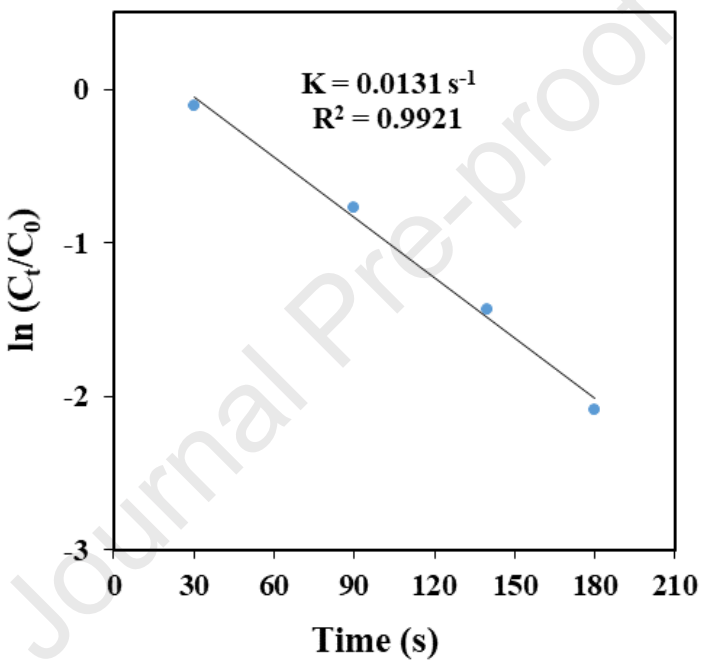

Figure 6. Plot of $-\ln(C_t/C_0)$ *vs*. reaction time in the catalytic reduction of 4-NP.

A comparison of the catalytic activity of Cu NPs@Fe_3O_4-LS catalyst with other previously reported catalysts in the reduction of MB, 4-NP, and CR in the presence of $NaBH_4$ is given in Table 4 [99-106]. The results confirm that Cu NPs@Fe_3O_4-LS catalyst shows high catalytic activity in the reduction reactions compared to the other catalysts.

Table 4. Comparison of Cu NPs@Fe_3O_4-LS catalyst with other reported catalysts in the reduction of MB, 4-NP and CR by $NaBH_4$.

Catalyst (mg)	Pollutant (M)	$NaBH_4$ (M)	Time	Ref.
Pd NPs@chitosan-MWCNT (4)	MB (1.0×10^{-4})	3 mg	Instantly	[99]
GA-Sch-Pd (5)	MB (1.0×10^{-5})	0.05	5 s	[100]
Pd-CS-g-C_3N_4 (5)	MB (1.0×10^{-5})	0.05	5 s	[101]
Pd/CS/γMnO_2 (8)	MB (1.3×10^{-5})	0.06	17 s	[102]
ZrO_2-Au nanocomposite (3)	MB (3.1×10^{-5})	0.053	20 s	[103]
Fe_3O_4-Ag (1)	MB (40 mg L^{-1})	0.1	18 min	[104]
Cu NPs@Fe_3O_4-LS (3)	MB (3.1×10^{-5})	0.053	Instantly	This work
Pd NPs@chitosan-MWCNT (4)	4-NP (1.0×10^{-4})	0.05	720 s	[99]
CS-CNTs-PdNPs (250)	4-NP (6.0×10^{-4})	0.5	900 s	[105]
CS-rGO-PdNPs (250)	4-NP (6.0×10^{-4})	0.5	1200 s	[105]
Cu/MnO_2 nanocomposite (7)	4-NP (2.5×10^{-3})	0.25	240 s	[106]
Cu NPs@Fe_3O_4-LS (7)	4-NP (2.5×10^{-3})	0.25	180 s	This work
Cu/MnO_2 nanocomposite (5)	CR (1.44×10^{-5})	0.053	87 s	[106]
Cu@SBA-15 (1)	CR (9.0×10^{-5})	0.2	7 min	[107]
Cu NPs@Fe_3O_4-LS (5)	CR (1.44×10^{-5})	0.053	40 s	This work

3.5 Biological ability of the Cu NPs@Fe_3O_4-LS

3.5.1 Antibacterial activity of Cu NPs@Fe_3O_4-LS

The main reason why NPs are considered as an alternative to antibiotics is that NPs can efficiently avoid the microbes, which play an antimicrobial role under severe microbial conditions. The widespread application of antibiotics has led to the emergence of many dangers to public health, such as superbugs, which do not respond to any present drug, and epidemics against which medicine has no defense. The development of novel and effective bactericidal compounds is important for combatting drug resistance and NPs have been recognized as promising compounds

to solve this difficulty. According to the results of ongoing research, the main methods underlying the antibacterial effects of NPs are as follows: 1) disruption of the bacterial cell membrane; 2) production of ROS; 3) penetration of the bacterial cell membrane; and 4) induction of intracellular antibacterial effects, including interactions with proteins and DNA [108]. The effect of antibacterial potency of Cu NPs@Fe_3O_4-LS on *S. aureus* and *E. coli* was investigated. The results are reported as MIC and MBC in Table 5.

Table 5. Antibacterial activities of Cu NPs@Fe_3O_4-LS.

Selected food related microorganisms (µg/mL)			
Catalyst	**Bacterial strain**	**MIC**	**MBC**
Cu NPs@Fe_3O_4-LS	*Escherichia coli*	66±2.64	132±5.29
Cu NPs@Fe_3O_4-LS	*Staphylococcus aureus*	32.66±1.52	65.33±3.05

3.5.2 DPPH radical scavenging prowess

DPPH is a kind of stable and hydrophile free radical applied as an antioxidant of plants extracts. An alcoholic solution of DPPH has a maximum absorbance at 515-517 nm owing to the presence of an unpaired electron. Electron and/or hydrogen transfer from reducing agents such as phenols to DPPH free radical and change them to a non-radical form leads to a reduction in DPPH absorption in this wavelength. Therefore, the antioxidant prowess of Cu NPs@Fe_3O_4-LS is shown by percentage of reduction in absorption content of DPPH solution in Cu NPs@Fe_3O_4-LS [109]. In Table 6, the antioxidant performance of Cu NPs@Fe_3O_4-LS and synthetic antioxidants against DPPH are shown using IC_{50}. A lower IC_{50} signifies a better antioxidant capability. As displayed in Table 6, the antioxidant activity of Cu NPs@Fe_3O_4-LS is good and significant. However, the antioxidant activity of Cu NPs@Fe_3O_4-LS is considerably lower than those of BHA and BHT.

Table 6. Antioxidant activity of Cu NPs@Fe_3O_4-LS compared to BHA[a] and BHT[b] synthetic antioxidants.

Substrate	DPPH[c]	RP[d]
Cu NPs@Fe_3O_4-LS	300.57±2.46	4543.33±7076
BHA	53.8±1.13	84.06±1.6
BHT	63.8±1.3	90.5±1.15

[a] Butylated hydroxyanisole.

[b] Butylated hydroxytoluene.

[c] Matching to IC_{50} (µg/mL).

[d] Reducing power = absorbance at 0.5 µg/mL.

3.5.3 Fe^{+3} reducing power

The reducing ability of Cu NPs@Fe_3O_4-LS displays its powerful antioxidant prowess towards Fe^{+3} ions. The antioxidant Cu NPs@Fe_3O_4-LS changes yellow colored Fe^{+3}/ferricyanide complex to blue colored Fe^{+2} complex. The reductive capability of NPs is enhanced with increasing concentrations which was established achieved using the corresponding λ_{max} value at 700 nm. Nonetheless, the reductive ability of Cu NPs@Fe_3O_4-LS is less in comparison with BHA and BHT. The experimental results are listed in Table 6 along with the amounts of synthetic antioxidants.

3.6 Recyclability of Cu NPs@Fe_3O_4-LS

One of the most significant issues in the synthesis of catalysts is the capability to recycle them. The easier the process of separating the catalysts from the reaction media, the greater the recyclability of that catalyst. The synthesized Cu NPs@Fe_3O_4-LS are simply separated by an external magnet because of their magnetic properties. The recyclability of Cu NPs@Fe_3O_4-LS in the catalytic reduction of 4-NP has been investigated. Upon the completion of the first cycle, Cu

NPs@Fe_3O_4-LS catalyst was easily separated from the reaction mixture *via* an external magnet, washed with water, dried and then reused in the next run. The same regeneration process was used for each run. The tests displayed that Cu NPs@Fe_3O_4-LS can be recycled and reused 4 times with no noteworthy decrease in performance (Figure S3). To address this issue, the TEM images of the recycled catalyst displayed in Figure S3 were used to determine its morphological and size changes. There are no significant changes in the morphology and size of the particles after the recycling tests (Figure S3). This provides strong evidence for the structural stability and durability of Cu NPs@Fe_3O_4-LS catalyst.

4. Conclusions

Plant extracts have been the subject of recent studies, and the number of research papers published in this area has exploded in the past eight years as a result of their widespread availability, cost-effectiveness, and environmental friendliness. Plants also contain the most efficient synthetic chemicals, which increases the rate of synthesis. Plant-mediated green synthesis of MNPs, being simple, efficient, rapid, reliable, and eco-friendly in nature, has gained an edge over traditional methods, which are expensive, toxic, and inefficient. This study demonstrated the synthesis of Cu NPs@Fe_3O_4-LS catalyst using *Filago arvensis* L. aqueous extract. Cu NPs@Fe_3O_4-LS were synthesized *via* the immobilization of Cu NPs on the magnetic lignosulfonate surface. The catalytic applications of Cu NPs@Fe_3O_4-LS in MB, CR, and 4-NP reduction at ambient temperature has been studied. In this study, the $NaBH_4$-mediated reduction of pollutants was catalyzed by highly active Cu NPs@Fe_3O_4-LS in an appropriate time. Furthermore, we report the antibacterial and antioxidant activity of Cu NPs@Fe_3O_4-LS. The results of the present study show that Cu NPs@Fe_3O_4-LS has antibacterial activity against *S. aureus* and *E. coli*. The results also

show that Fe_3O_4-LS supported Cu NPs can improve the catalytic performance, providing an economic and environmental protection application for MB, CR, and 4-NP reduction. The catalyst exhibited significant catalytic activity with high crystallinity, sufficient Cu loading, magnetic separability, and nanoscale size. The Cu NPs@Fe_3O_4-LS catalyst, which could be completely separated using a magnet, maintains high catalytic activity after four cycles. Clearly, this novel catalyst has potential applications in catalysis and wastewater remediation in the future.

Conflicts of interest

There are no conflicts to declare.

Acknowledgements

The supports from Iranian Nano Council and the University of Qom are appreciated. This research was also supported by the National Research Foundation of Korea (NRF) funded by the Ministry of Science and ICT (2020M2D8A206983011, 2021R1A4A3027878, and 2022R111A1A0106757211). Furthermore, the financial supports of the Basic Science Research Program (2017R1A2B3009135) through the National Research Foundation of Korea and Rural Development Administration (PJ01706703) are appreciated. We also gratefully acknowledge the financial support provided by Zhejiang Normal University (Grant No. YS304221928), Natural Science Foundation of Zhejiang Province (Nos. LD21E080001) and Zhejiang Provincial Ten Thousand Talent Program (ZJWR0302055).

References

[1] Z. Pan, B. Zeng, H. Lin, J. Teng, H. Zhang, H. Hong, M. Zhang, Fundamental thermodynamic mechanisms of membrane fouling caused by transparent exopolymer particles (TEP) in water treatment, Sci. Total Environ. 820 (2022) 153252.

[2] L. Han, C. Chen, L. Shen, H. Lin, B. Li, Z. Huang, Y. Xu, R. Li, H. Hong, Novel membranes with extremely high permeability fabricated by 3D printing and nickel coating for oil/water separation, J. Mater. Chem. A 10 (2022) 12055-12061.

[3] L. Zhang, Y. Xu, H. Liu, Y. Li, S. You, J. Zhao, J. Zhang, Effects of coexisting Na^{+}, Mg^{2+} and Fe^{3+} on nitrogen and phosphorus removal and sludge properties using $A^{2}O$ process, J. Water Process. Eng. 44 (2021) 102368.

[4] H. Liu, J. Yang, Y. Jia, Z. Wang, M. Jiang, K. Shen, H. Zhao, Y. Guo, Y. Guo, L. Wang, S. Dai, W. Zhan, Significant improvement of catalytic performance for chlorinated volatile organic compound oxidation over RuO_x supported on acid-etched Co_3O_4, Environ. Sci. Technol. 55(15) (2021) 10734-10743.

[5] Y. Orooji, N. Han, Z. Nezafat, N. Shafiei, Z. Shen, M. Nasrollahzadeh, H. Karimi-Maleh, R. Luque, A. Bokhari, J. J. Klemeš, Valorisation of nuts biowaste: Prospects in sustainable bio (nano) catalysts and environmental applications, J. Clean. Prod. 347 (2022) 131220.

[6] Z. Xu, J. Shen, Y. Qu, H. Chen, X. Zhou, H. Hong, H. Sun, H. Lin, W. Deng, F. Wu, Using simple and easy water quality parameters to predict trihalomethane occurrence in tap water, Chemosphere 286 (2022) 131586.

[7] M.I. Din, R. Khalid, Z. Hussain, T. Hussain, A. Mujahid, J. Najeeb, F. Izhar, Nanocatalytic

461 assemblies for catalytic reduction of nitrophenols: a critical review, Crit. Rev. Anal. Chem. 50
462 (2020) 322-338.

463 [8] H.M.A. Sharif, A. Mahmood, H.-Y. Cheng, R. Djellabi, J. Ali, W.-L. Jiang, S.-S. Wang,
464 M.R. Haider, N. Mahmood, A.-J. Wang, Fe_3O_4 nanoparticles coated with EDTA and Ag
465 nanoparticles for the catalytic reduction of organic dyes from wastewater, ACS Appl. Nano Mater.
466 2 (2019) 5310-5319.

467 [9] G. Palani, A. Arputhalatha, K. Kannan, S.K. Lakkaboyana, M.M. Hanafiah, V. Kumar,
468 R.K. Marella, Current trends in the application of nanomaterials for the removal of pollutants from
469 industrial wastewater treatment—a review, Molecules 26 (2021) 2799.

470 [10] R. Keyikoglu, A. Khataee, H. Lin, Y. Orooji, Vanadium(V)-doped ZnFe LDH for
471 enhanced sonocatalytic degradation of pymetrozine, Chem. Eng. J. 434 (2022) 134730.

472 [11] H. Sohrabi, M.R. Majidi, O. Arbabzadeh, P. Khaaki, S. Pourmohammad, A. Khataee, Y.
473 Orooji, Recent advances in the highly sensitive determination of zearalenone residues in water and
474 environmental resources with electrochemical biosensors, Environ. Res. 204 (2022) 112082.

475 [12] A. Turki Jalil, H. Emad Al. Qurabiy, S. Hussain Dilfy, S. Oudah Meza, S. Aravindhan,
476 M.M. Kadhim, A.M. Aljeboree, CuO/ZrO_2 nanocomposites: facile synthesis, characterization and
477 photocatalytic degradation of tetracycline antibiotic, J. Nanostruct. 11(2) (2021) 333-341

478 [13] S.B. Khan, Metal nanoparticles containing chitosan wrapped cellulose nanocomposites for
479 catalytic hydrogen production and reduction of environmental pollutants, Carbohydr. Polym. 242
480 (2020) 116286.

481 [14] A. Khalil, N. Ali, A. Khan, A.M. Asiri, T. Kamal, Catalytic potential of cobalt oxide and

agar nanocomposite hydrogel for the chemical reduction of organic pollutants, Int. J. Biol. Macromol. 164 (2020) 2922-2930.

[15] M. Hachemaoui, A. Mokhtar, A. Mekki, F. Zaoui, S. Abdelkrim, S. Hacini, B. Boukoussa, Composites beads based on Fe_3O_4@MCM-41 and calcium alginate for enhanced catalytic reduction of organic dyes, Int. J. Biol. Macromol. 164 (2020) 468-479.

[16] D. Habibi, M. Nasrollahzadeh, H. Sahebekhtiari, Green synthesis of formamides using the Natrolite zeolite as a natural, efficient and recyclable catalyst, J. Mol. Catal. A Chem. 378 (2013) 148-155.

[17] Y. Orooji, K. Pakzad, M. Nasrollahzadeh, Lignosulfonate valorization into a Cu-containing magnetically recyclable photocatalyst for treating wastewater pollutants in aqueous media, Chemosphere 305 (2022) 135180.

[18] Y. Orooji, A. Alizadeh, E. Ghasali, M.R. Derakhshandeh, M. Alizadeh, M. Shahedi Asl, T. Ebadzadeh, Co-reinforcing of mullite-tin-cnt composites with ZrB_2 and TiB_2 compounds, Ceram. Int. 45(16) (2019) 20844-20854.

[19] Y. Orooji, M.R. Derakhshandeh, E. Ghasali, M. Alizadeh, M. Shahedi Asl, T. Ebadzadeh, Effects of ZrB_2 reinforcement on microstructure and mechanical properties of a spark plasma sintered mullite-cnt composite, Ceram. Int. 45(13) (2019) 16015-16021.

[20] G. Wu, W. Zhu, Q. He, Z. Feng, T. Huang, L. Zhang, S. Schmidt, A. Godfrey, X. Huang, 2D and 3D orientation mapping in nanostructured metals: A review, Nano Mater. Sci. 2(1) (2020) 50-57.

[21] M. Ding, G. Chen, W. Xu, C. Jia, H. Luo, Bio-inspired synthesis of nanomaterials and

503 smart structures for electrochemical energy storage and conversion, Nano Mater. Sci. 2(3) (2020)
504 264-280.

505 [22] K. Yorseng, S. Siengchin, B. Ashok, A.V. Rajulu, Nanocomposite egg shell powder with
506 in situ generated silver nanoparticles using inherent collagen as reducing agent, J. Bioresour.
507 Bioprod. 5(2) (2020) 101-107.

508 [23] B. Ashok, N. Hariram, Suchart Siengchin, A. Varada Rajulu, Modification of tamarind
509 fruit shell powder with in situ generated copper nanoparticles by single step hydrothermal method,
510 J. Bioresour. Bioprod. 5(3) (2020) 180-185.

511 [24] S. Naghdi, K.Y. Rhee, B. Jaleh, S.J. Park, Altering the structure and properties of iron
512 oxide nanoparticles and graphene oxide/iron oxide composites by urea, Appl. Surf. Sci. 364 (2016)
513 686-693.

514 [25] Z. Cheng, J. Meng, X. Wang, Preparation of wood-based filter loaded with Ag
515 nanoparticles and its catalytic degradation performance on organic dye, J. Forest. Eng. 5(6) (2020)
516 94-98.

517 [26] H. Xia, J. An, W. Zhang, C. Ge, S. Zuo, Effect of the metal-support interaction on catalytic
518 oxidation performances of HMF on Ag nanoparticles, J. Forest. Eng. 5(6) (2020) 88-93.

519 [27] Y. Zhang, L. Wei, L. Lu, L. Gan, M. Pan, Adsorption-photocatalytic properties of cellulose
520 nanocrystal supported ZnO nanocomposites, J. Forest. Eng. 5(3) (2020) 29-35.

521 [28] T. Li, D. Shang, S. Gao, B. Wang, H. Kong, G. Yang, W. Shu, P. Xu, G. Wei, Two-
522 dimensional material-based electrochemical sensors/biosensors for food safety and biomolecular
523 detection, Biosensors 12(5) (2022) 314.

[29] M. Liu, C. Li, Y. Zhang, Q. An, M. Yang, T. Gao, C. Mao, B. Liu, H. Cao, X. Xu, Z. Said, S. Debnath, M. Jamil, H.M. Ali, S. Sharma, Cryogenic minimum quantity lubrication machining: from mechanism to application, Front. Mech. Eng. 16(4) (2021) 649-697.

[30] T. Gao, Y. Zhang, C. Li, Y. Wang, Q. An, B. Liu, Z. Said, S. Sharma, Grindability of carbon fiber reinforced polymer using CNT biological lubricant, Sci. Rep. 11 (2021) Article number: 22535.

[31] W.-F. Lai, Non-conjugated polymers with intrinsic luminescence for drug delivery, J. Drug. Deliv. Sci. Technol. 59 (2020) 101916.

[32] G. Liu, R. Nie, Y. Liu, A. Mehmood, Combined antimicrobial effect of bacteriocins with other hurdles of physicochemic and microbiome to prolong shelf life of food: A review, Sci. Total Environ. 825 (2022) 154058.

[33] W. Yang, W. Liu, X. Li, J. Yan, W. He, Turning chiral peptides into a racemic supraparticle to induce the self-degradation of MDM2, J. Adv. Res. (2022) https://doi.org/10.1016/j.jare.2022.05.009.

[34] J. Yan, Y. Yao, S. Yan, R. Gao, W. Lu, W. He, Chiral protein supraparticles for tumor suppression and synergistic immunotherapy: An enabling strategy for bioactive supramolecular chirality construction, Nano Lett. 20(8) (2020) 5844-5852.

[35] M. Yang, C. Li, Z. Said, Y. Zhang, R. Li, S. Debnath, H.M. Ali, T. Gao, Y. Long, Semiempirical heat flux model of hard-brittle bone material in ductile microgrinding, J. Manuf. Process. 71 (2021) 501-514.

[36] L. Zhu, G. Liang, C. Guo, M. Xu, M. Wang, C. Wang, Z. Zhang, M. Du, A new strategy

for the development of efficient impedimetric tobramycin aptasensors with metallo-covalent organic frameworks (MCOFs), Food Chem. 366 (2022) 130575.

[37] Z. Shen, X. Xing, S. Wang, M. Lv, J. Li, T. Li, Effect of K-modified blue coke-based activated carbon on low temperature catalytic performance of supported Mn-Ce/activated carbon, ACS Omega 7(10) (2022) 8798-8807.

[38] X. Cui, C. Li, W. Ding, Y. Chen, C. Mao, X. Xu, B. Liu, D. Wang, H.N. Li, Y. Zhang, Z. Said, S. Debnath, M. Jamil, H.M. Ali, S. Sharma, Minimum quantity lubrication machining of aeronautical materials using carbon group nanolubricant: from mechanisms to application, Chinese J. Aeronaut. (2021), doi: https://doi.org/10.1016/j.cja.2021.08.011.

[39] Y. Zhang, H.N. Li, C. Li, C. Huang, H.M. Ali, X. Xu, C. Mao, W. Ding, X. Cui, M. Yang, T. Yu, M. Jamil, M.K. Gupta, D. Jia, Z. Said, Nano-enhanced biolubricant in sustainable manufacturing: From processability to mechanisms, Friction 10 (2022) 803-841.

[40] J.S. Xia, A. Majdi, D. Toghraie, Molecular dynamics simulation of friction process in atomic structures with spherical nanoparticles, Solid State Commun. 346 (2022) 114717.

[41] S. Chupradit, A.T. Jalil, Y. Enina, D.A. Neganov, M.S. Alhassan, S. Aravindhan, A. Davarpanah, Use of organic and copper-based nanoparticles on the turbulator installment in a shell tube heat exchanger: A CFD-based simulation approach by using nanofluids, J. Nanomater. 2021 (2021) Article ID 3250058.

[42] D. Bokov, A. Turki Jalil, S. Chupradit, W. Suksatan, M.J. Ansari, I.H. Shewael, G.H. Valiev, E. Kianfar, Nanomaterial by sol-gel method: Synthesis and application. Adv. Mater. Sci. Eng. 2021 (2021) Article ID 5102014.

[43] R.O. Saleh, D.O. Bokov, M.N. Fenjan, W.K. Abdelbasset, U.S. Altimari, A.T. Jalil, L. Thangavelu, W. Suksatan, Y. Cao, Application of aluminum nitride nanotubes as a promising nanocarriers for anticancer drug 5-aminosalicylic acid in drug delivery system, J. Mol. Liq. 352 (2022) 118676.

[44] S.A. Jasim, J.M. Hadi, M.J.C. Opulencia, Y.S. Karim, A.B. Mahdi, M.M. Kadhim, D.O. Bokov, A.T. Jalil, Y.F. Mustafa, K.T. Falih, MXene/metal and polymer nanocomposites: preparation, properties, and applications, J. Alloys Compd. 917 (2022) 165404.

[45] X. Hu, A.H. Derakhshanfard, I. Khalid, A.T. Jalil, M.J.C. Opulencia, R.B. Dehkordi, D. Toghraie, M. Hekmatifar, R. Sabetvand, The microchannel type effects on water-Fe_3O_4 nanofluid atomic behavior: Molecular dynamics approach, J. Taiwan Inst. Chem. Eng. 135 (2022) 104396.

[46] D.O. Bokov, A.T. Jalil, F.H. Alsultany, M.Z. Mahmoud, W. Suksatan, S. Chupradit, M.T. Qasim, P. Delir Kheirollahi Nezhad, Ir-decorated gallium nitride nanotubes as a chemical sensor for recognition of mesalamine drug: a DFT study, Mol. Simul. 48(5) (2022) 438-447.

[47] K., Hachem, S. A., Jasim, M. E., Al- Gazally, Y., Riadi, G., Yasin, A.T. Jalil, M.M. Abdulkadhm, M.M. Saleh, M.N. Fenjan, Y.F. Mustafa, A.D. Khalaji, Adsorption of Pb(II) and Cd(II) by magnetic chitosan- salicylaldehyde Schiff base: Synthesis, characterization, thermal study and antibacterial activity, J. Chin. Chem. Soc. 69(3) (2022) 512-521.

[48] R. Kartika, F.H. Alsultany, A.T. Jalil, M.Z. Mahmoud, M.N. Fenjan, H. Rajabzadeh, $Ca_{12}O_{12}$ nanocluster as highly sensitive material for the detection of hazardous mustard gas: Density-functional theory, Inorg. Chem. Commun. 137 (2022) 109174.

[49] N. Ngafwan, H. Rasyid, E.S. Abood, W.K. Abdelbasset, S.G. Al-Shawi, D. Bokov, A. T. Jalil, Study on novel fluorescent carbon nanomaterials in food analysis. Food Sci. Technol. 42

(2022) e37821.

[50] Z. Taherian, A. Khataee, N. Han, Y. Orooji, Hydrogen production through methane reforming processes using promoted-Ni/mesoporous silica: A review. J. Ind. Eng. Chem. 107 (2022) 20-30.

[51] Z. Taherian, V. Shahed Gharahshiran, A. Khataee, Y. Orooji, Synergistic effect of freeze-drying and promoters on the catalytic performance of Ni/MgAl layered double hydroxide, Fuel 311 (2022) 122620.

[52] S.A. Jasim, M.J. Ansari, H.S. Majdi, M.J.C. Opulencia, K. F. Uktamov, Nanomagnetic salamo-based-Pd(0) complex: an efficient heterogeneous catalyst for Suzuki-Miyaura and Heck cross-coupling reactions in aqueous medium, J. Mol. Struct. 1261, (2022) 132930.

[53] X. Zhao, L. Lv, B. Pan, W. Zhang, S. Zhang, Q. Zhang, Polymer-supported nanocomposites for environmental application: a review, Chem. Eng. J. 170 (2011) 381-394.

[54] A. Al-Nayili, H.S. Majdi, T.M. Albayati, N.M.C. Saady, Formic acid dehydrogenation using noble-metal nanoheterogeneous catalysts: Towards sustainable hydrogen-based energy, Catalysts 12(3) (2022) 324.

[55] Y. Zhang, Y. Zhou, Y. Zhao, C. Liu, Recent progresses in the size and structure control of MOF supported noble metal catalysts, Catal. Today. 263 (2016) 61-68.

[56] P. Veerakumar, K.-C. Lin, An overview of palladium supported on carbon-based materials: Synthesis, characterization, and its catalytic activity for reduction of hexavalent chromium, Chemosphere 253 (2020) 126750.

[57] O.D. Salahdin, A. Majdi, M.J. Opulencia, T.Z. Taban, A.T. Hammid, X. Zhao, Oxygen

609 reduction reaction on metal-doped nanotubes and nanocages for fuel cells, Ionics 28 (2022) 3409-
610 3419.

611 [58] Y. He, H. Lin, Y. Dong, B. Li, L. Wang, S. Chu, M. Luo, J. Liu, Zeolite supported Fe/Ni
612 bimetallic nanoparticles for simultaneous removal of nitrate and phosphate: synergistic effect and
613 mechanism, Chem. Eng. J. 347 (2018) 669-681.

614 [59] S.A. Jasim, M.J. Catalan Opulencia, A. Majdi, D.Z. Yusupova, Y.F. Mustafa, A.T.
615 Hammid, P. Delir Kheirollahi Nezhad, Investigation of crotonaldehyde adsorption on pure and Pd-
616 decorated gan nanotubes: A density functional theory study, Solid State Commun. 348-349 (2022)
617 114741.

618 [60] Y. Liu, C. Jin, Z. Yang, G. Wu, G. Liu, Z. Kong, Recent advances in lignin-based porous
619 materials for pollutants removal from wastewater, Int. J. Biol. Macromol. 187 (2021) 880-891.

620 [61] C. Wang, S.S. Kelley, R.A. Venditti, Lignin- based thermoplastic materials,
621 ChemSusChem. 9 (2016) 770-783.

622 [62] H. Wang, Y. Pu, A. Ragauskas, B. Yang, From lignin to valuable products-strategies,
623 challenges, and prospects, Bioresour. Technol. 271 (2019) 449-461.

624 [63] A.J. Ragauskas, G.T. Beckham, M.J. Biddy, R. Chandra, F. Chen, M.F. Davis, B.H.
625 Davison, R.A. Dixon, P. Gilna, M. Keller, P. Langan, A.K. Naskar, J.N. Saddler, T.J. Tschaplinski,
626 G.A. Tuskan, C.E. Wyman, Lignin valorization: improving lignin processing in the biorefinery,
627 Science 344(6185) (2014) 1246843.

628 [64] H. Li, Y. Liang, P. Li, C. He, Conversion of biomass lignin to high-value polyurethane: A
629 review, J. Bioresour. Bioprod. 5 (2020) 163-179.

[65] S. Padalkar, J.R. Capadona, S.J. Rowan, C. Weder, Y.-H. Won, L.A. Stanciu, R.J. Moon, Natural biopolymers: novel templates for the synthesis of nanostructures, Langmuir 26 (2010) 8497-8502.

[66] A.V. Rane, K. Kanny, V.K. Abitha, S. Thomas, Methods for synthesis of nanoparticles and fabrication of nanocomposites, In: Synthesis of Inorganic Nanomaterials, Elsevier, 2018: pp. 121-139.

[67] X. Ji, M. Guo, L. Zhu, W. Du, H. Wang, Synthesis mechanism of an environment-friendly sodium lignosulfonate/chitosan medium-density fiberboard adhesive and response of bonding performance to synthesis mechanism, Materials 13 (2020) 5697.

[68] N. Chokhachi Zadeh Moghadam, S.A. Jasim, F. Ameen, D.H. Alotaibi, M.A.L. Nobre, H. Sellami, M. Khatami, Nickel oxide nanoparticles synthesis using plant extract and evaluation of their antibacterial effects on *Streptococcus mutans*, Bioprocess Biosyst. Eng. 45(7) (2022) 1201-1210.

[69] F. Ameen, K.S. Al-Maary, A. Almansob, S. AlNadhari, Antioxidant, antibacterial and anticancer efficacy of *Alternaria chlamydospora*-mediated gold nanoparticles, Appl. Nanosci. (2022). https://doi.org/10.1007/s13204-021-02047-4.

[70] F. Ameen, Optimization of the synthesis of fungus-mediated bi-metallic Ag-Cu nanoparticles, Appl. Sci. 12(3) (2022) 1384.

[71] H. Sonbol, S. AlYahya, F. Ameen, K. Alsamhary, S. Alwakeel, S. Al-Otaibi, S. Korany, Bioinspired synthesize of CuO nanoparticles using *Cylindrospermum stagnale* for antibacterial, anticancer and larvicidal applications, Appl. Nanosci. (2021). https://doi.org/10.1007/s13204-021-01940-2.

[72] F. Ameen, A.A. Al-Homaidan, A. Al-Sabri, A. Almansob, S. AlNAdhari, Anti-oxidant, anti-fungal and cytotoxic effects of silver nanoparticles synthesized using marine fungus *Cladosporium halotolerans*, Appl. Nanosci. (2021). https://doi.org/10.1007/s13204-021-01874-9.

[73] N.M. Al-Enazi, F. Ameen, K. Alsamhary, T. Dawoud, F. Al-Khattaf, S. AlNadhari, Tin oxide nanoparticles (SnO_2-NPs) synthesis using *Galaxaura elongata* and its anti-microbial and cytotoxicity study: a greenery approach, Appl Nanosci (2021). https://doi.org/10.1007/s13204-021-01828-1.

[74] H. Sonbol, F. Ameen, S. AlYahya, A. Almansob, S. Alwakeel, *Padina boryana* mediated green synthesis of crystalline palladium nanoparticles as potential nanodrug against multidrug resistant bacteria and cancer cells, Sci. Rep. 11 (2021) 5444.

[75] S. AlNadhari, N.M. Al-Enazi, F. Alshehrei, F. Ameen, A review on biogenic synthesis of metal nanoparticles using marine algae and its applications, Environ. Res. 194 (2021) 110672.

[76] M. Isacfranklin, T. Dawoud, F. Ameen, G.Ravi, R. Yuvakkumar, P. Kumar, S.I. Hong, D. Velauthapillai, B. Saravanakumar, Synthesis of highly active biocompatible ZrO_2 nanorods using a bioextract, Ceram. Int. 46(16) (2020) 25915-25920.

[77] Y. Kishore Mohanta, S. Kumar Panda, A. Syed, F. Ameen, A. Kumar Bastia, T. Kumar Mohanta, Bio-inspired synthesis of silver nanoparticles from leaf extracts of *Cleistanthus collinus* (Roxb.): its potential antibacterial and anticancer activities, IET Nanobiotechnol. 12(3) (2018) 343-348.

[78] M. Khatami, F. Mosazade, M. Raeisi, M. Ghasemi, Z. Fazli, K. Arefkia, R.S. Varma, F. Borhani, S. Khatami, Simplification of gold nanoparticle synthesis with low cytotoxicity using a greener approach: opening up new possibilities, RSC Adv. 11 (2021) 3288-3294.

[79] Y. Cao, H.Q. Alijani, M. Khatami, F. Bagheri-Baravati, S. Iravani, F. Sharifi, K-doped ZnO nanostructures: biosynthesis and parasiticidal application, J. Mater. Res. Technol. 15 (2021) 5445-5451.

[80] M.H.S. Surmaghi, Y.A.G.H. Amin, Z. Mahmoodi, Survey of iranian plants for saponins alkaloids flavonoids and tannins. IV, DARU J. Pharm. Sci. 2 (1992) 1-11.

[81] M. Galbany-Casals, S. Andrés-Sánchez, N. Garcia-Jacas, A. Susanna, E. Rico, M.M. Martínez-Ortega, How many of Cassini anagrams should there be? Molecular systematics and phylogenetic relationships in the Filago group (Asteraceae, Gnaphalieae), with special focus on the genus Filago, Taxon. 59 (2010) 1671-1689.

[82] M. Nasrollahzadeh, N.S.S. Bidgoli, Z. Issaabadi, Z. Ghavamifar, T. Baran, R. Luque, *Hibiscus Rosasinensis* L. aqueous extract-assisted valorization of lignin: Preparation of magnetically reusable Pd NPs@Fe_3O_4-lignin for Cr(VI) reduction and Suzuki-Miyaura reaction in eco-friendly media, Int. J. Biol. Macromol. 148 (2020) 265-275.

[83] F. Jalilian, A. Chahardoli, K. Sadrjavadi, A. Fattahi, Y. Shokoohinia, Green synthesized silver nanoparticle from *Allium ampeloprasum* aqueous extract: Characterization, antioxidant activities, antibacterial and cytotoxicity effects, Adv. Powder Technol. 31 (2020) 1323-1332.

[84] M.M. Karimkhani, D. Salarbashi, S.S. Sefidy, A. Mohammadzadeh, Effect of extraction solvents on lipid peroxidation, antioxidant, antibacterial and antifungal activities of Berberis orthobotrys Bienerat ex CK Schneider, J. Food Meas. Charact. 13 (2019) 357-367.

[85] I. Golonka, S. Wilk, W. Musiał, The Influence of UV Radiation on the Degradation of Pharmaceutical Formulations Containing Quercetin, Molecules 25 (2020) 5454.

[86] Z. Nezafat, M. Nasrollahzadeh, Biosynthesis of Cu/Fe_3O_4 nanoparticles using Alhagi camelorum aqueous extract and their catalytic activity in the synthesis of 2-imino-3-aryl-2, 3-dihydrobenzo[*d*]oxazol-5-ol derivatives, J. Mol. Struct. 1228 (2021) 129731.

[87] X. Ji, M. Guo, L. Zhu, W. Du, H. Wang, Synthesis mechanism of an environment-friendly sodium lignosulfonate/chitosan medium-density fiberboard adhesive and response of bonding performance to synthesis mechanism, Materials 13 (2020) 5697.

[88] M. Amiri, M. Salavati-Niasari, A. Pardakhty, M. Ahmadi, A. Akbari, Caffeine: A novel green precursor for synthesis of magnetic $CoFe_2O_4$ nanoparticles and pH-sensitive magnetic alginate beads for drug delivery, Mater. Sci. Eng. C 76 (2017) 1085-1093.

[89] S. Zinatloo-Ajabshir, M. Salavati-Niasari, Preparation of magnetically retrievable $CoFe_2O_4$@SiO_2@$Dy_2Ce_2O_7$ nanocomposites as novel photocatalyst for highly efficient degradation of organic contaminants, Compos. B. Eng. 174 (2019) 106930.

[90] P. Mondal, A. Sinha, N. Salam, A.S. Roy, N.R. Jana, S.M. Islam, Enhanced catalytic performance by copper nanoparticle-graphene based composite, RSC Adv. 3 (2013) 5615-5623.

[91] S. Megarajan, F. Ameen, D. Singaravelu, M.A. Islam, A. Veerappan, Synthesis of N-myristoyltaurine stabilized gold and silver nanoparticles: Assessment of their catalytic activity, antimicrobial effectiveness and toxicity in zebrafish, Environ. Res. 212(Part A) (2022) 113159.

[92] A. Khataee, A. Fazli, F. Zakeri, S. Woo Joo, Synthesis of a high-performance Z-scheme 2D/2D WO_3@CoFe-LDH nanocomposite for the synchronic degradation of the mixture azo dyes by sonocatalytic ozonation process, J. Ind. Eng. Chem. 89 (2020) 301-315.

[93] A. Khataee, D. Kalderis, P. Gholami, A. Fazli, M. Moschogiannaki, V. Binas, M. Lykaki,

716 M. Konsolakis, Cu_2O-CuO@biochar composite: Synthesis, characterization and its efficient
717 photocatalytic performance, Appl. Surf. Sci. 498 (2019) 143846.

718 [94] Z. Ansarian, A. Khataee, S. Arefi-Oskoui, Y. Orooji, H. Lin, Ultrasound-assisted catalytic
719 activation of peroxydisulfate on Ti_3GeC_2 MAX phase for efficient removal of hazardous
720 pollutants, Mater. Today Chem. 24 (2022) 100818.

721 [95] S. Arefi-Oskoui, A. Khataee, S. Jabbarvand Behrouz, V. Vatanpour, S. Haddadi
722 Gharamaleki, Y. Orooji, M. Safarpour, Development of MoS_2/O-MWCNTs/PES blended
723 membrane for efficient removal of dyes, antibiotic, and protein, Sep. Purif. Technol. 280 (2022)
724 119822.

725 [96] D. Indhira, M. Krishnamoorthy, F. Ameen, S.A. Bhat, K. Arumugam, S. Ramalingam, S.R.
726 Priyan, G.S. Kumar, Biomimetic facile synthesis of zinc oxide and copper oxide nanoparticles
727 from *Elaeagnus indica* for enhanced photocatalytic activity, Environ. Res. 212(Part C) (2019)
728 113323.

729 [97] F. Ameen, T. Dawoud, S. AlNadhari, Ecofriendly and low-cost synthesis of ZnO
730 nanoparticles from *Acremonium potronii* for the photocatalytic degradation of azo dyes, Environ.
731 Res. 202 (2021) 111700.

732 [98] M.M. Aljumaily, N.S. Ali, A.E. Mahdi, H.M. Alayan, M. AlOmar, M.M. Hameed, B.
733 Ismael, Q.F. Alsalhy, M.A. Alsaadi, H.S. Majdi, Z.B. Mohammed, Modification of
734 poly(vinylidene fluoride-co-hexafluoropropylene) membranes with DES-functionalized carbon
735 nanospheres for removal of methyl orange by membrane distillation, Water 14(9) (2022) 1396.

736 [99] I. Sargin, T. Baran, G. Arslan, Environmental remediation by chitosan-carbon nanotube
737 supported palladium nanoparticles: Conversion of toxic nitroarenes into aromatic amines,

738 degradation of dye pollutants and green synthesis of biaryls, Sep. Purif. Technol. 247 (2020)
739 116987.

740 [100] T. Baran, A. Menteş, Production of palladium nanocatalyst supported on modified gum
741 arabic and investigation of its potential against treatment of environmental contaminants,
742 International J. Biol. Macromol. 161 (2020) 1559-1567.

743 [101] N.Y. Baran, T. Baran, M. Çalışkan, Production of Pd nanoparticles embedded on micro-
744 sized chitosan/graphitic carbon nitride hybrid spheres for treatment of environmental pollutants in
745 aqueous medium, Ceram. Int. 47(19) (2021) 27736-27747.

746 [102] M. Çalışkan, T. Baran, Palladium nanoparticles embedded over chitosan/γMnO_2 composite
747 hybrid microspheres as heterogeneous nanocatalyst for effective reduction of nitroarenes and
748 organic dyes in water, J. Organomet. Chem. 237(2) (2022) 122284.

749 [103] S.M. Anis, S.H. Hashemi, A. Nasri, M. Sajjadi, M. Eslamipanah, B. Jaleh, Decorated ZrO_2
750 by Au nanoparticles as a potential nanocatalyst for the reduction of organic dyes in water, Inorg.
751 Chem. Commun. 141 (2022) 109489.

752 [104] Y. Liu, Y.Y. Zhang, Q.W. Kou, Y. Chen, D.L. Han, D.D. Wang, Z.Y. Lu, L. Chen, J.H.
753 Yang, S. Xing, Eco-friendly seeded Fe_3O_4-Ag nanocrystals: A new type of highly efficient and
754 low cost catalyst for methylene blue reduction, RSC Adv. 8 (2018) 2209-2218.

755 [105] J. Zhu, X. Zhang, Z. Qin, L. Zhang, Y. Ye, M. Cao, L. Gao, T. Jiao, Preparation of PdNPs
756 doped chitosan-based composite hydrogels as highly efficient catalysts for reduction of 4-
757 nitrophenol, Colloids Surf. A Physicochem. Eng. Asp. 611 (2021) 125889.

[106] M. Nasrollahzadeh, M. Sajjadi, S.M. Sajadi, Biosynthesis of copper nanoparticles supported on manganese dioxide nanoparticles using *Centella asiatica* L. leaf extract for the efficient catalytic reduction of organic dyes and nitroarenes, Chin. J. Catal. 39(1) (2018) 109-117.

[107] B. K. Ghosh, S. Hazra, B. Naik, N. N. Ghosh, Preparation of Cu nanoparticle loaded SBA-15 and their excellent catalytic activity in reduction of variety of dyes, Powder Technol. 269 (2015) 371-378.

[108] L. Wang, C. Hu, L. Shao, The antimicrobial activity of nanoparticles: present situation and prospects for the future, Int. J. Nanomedicine 12 (2017) 1227-1249.

[109] M.M. Karimkhani, R. Shaddel, M.H.H. Khodaparast, M. Vazirian, S. Piri-Gheshlaghi, Antioxidant and antibacterial activity of safflower (*Carthamus tinctorius* L.) extract from four different cultivars, Qual. Assur. Saf. Crop. Foods 8 (2016) 565-574.

Highlights:

- Facile synthesis of magnetic lignosulfonate supported copper nanoparticles.
- Efficient reduction of MB, CR and 4-NP using Cu NPs@Fe_3O_4-LS catalyst.
- Characterization of catalyst by FTIR, XRD, VSM, (HR)TEM, TG/DTA, EDS and XPS.
- The catalyst can be reused at least four times with low loss of catalytic ability.
- The antibacterial/antioxidant activities of Cu NPs@Fe_3O_4-LS were investigated.

Declaration of interests

☒ The authors declare that they have no known competing financial interests or personal relationships that could have appeared to influence the work reported in this paper.

☐The authors declare the following financial interests/personal relationships which may be considered as potential competing interests: